Nitric Oxide 82 (2019) 48–58

Contents lists available at ScienceDirect

Nitric Oxide

journal homepage: www.elsevier.com/locate/yniox

Nitric oxide regulates intussusceptive-like angiogenesis in wound repair in chicken embryo and transgenic zebrafish models

Selvaraj Vimalraj[a,b], Sivakamasundari Pichu[b], Thyagarajan Pankajam[b], Kasiviswanathan Dharanibalan[b], Valentin Djonov[c], Suvro Chatterjee[b,*]

[a] Centre for Biotechnology, Anna University, Chennai-600025, India
[b] Vascular Biology Lab, AU-KBC Research Centre and Department of Biotechnology, MIT Campus, Anna University, Chennai, India
[c] Institute of Anatomy, University of Berne, Buehlstrasse 26, CH-3012 Berne, Switzerland

ARTICLE INFO

Keywords:
Intussusceptive angiogenesis
Nitric oxide
Wound healing
Chorioallantoic membrane
Tumor endothelial marker 8

ABSTRACT

Angiogenesis is the formation of new blood vessels that occurs by two distinct processes following sprouting angiogenesis (SA) and intussusceptive angiogenesis (IA). Nitric oxide (NO) is known for its pro-angiogenic functions. However, no clear mechanisms are delineated on its role in promoting angiogenesis in reparative wound healing. We propose that NO regulates SA to IA transition and vice versa in wound milieu. We have used three models which include a new chick embryo extra-vasculature (CEV) burn wound model, adult Tie2-GFP transgenic Zebrafish caudal fin regeneration model and Zebrafish skin wound model to study the mechanisms underlying behind the role of NO in wound healing. Wounds created in CEV were treated with NO donor (Spermine NONOate (SPNO)), NOS inhibitor (L-nitro-L-arginine-methyl ester (L-NAME)), $NaNO_2$, $NaNO_3$, and beetroot juice, a nitrite-rich juice respectively and the pattern of wound healing was assessed. Morphological and histological techniques tracked the wound healing at the cellular level, and the molecular changes were investigated by using real-time RT-PCR gene expression analysis. The result concludes that NO donor promotes wound healing by activating SA at an early phase of healing while NOS inhibitor induces wound healing via IA. At the later phase of wound healing NO donor followed IA while NOS inhibitor failed to promote wound repair. The current work underpinned a differential regulation of NO on angiogenesis in wound milieu and this study would provide new insights in designing therapeutics for promoting wound repair.

1. Introduction

The wound is a loss or breaking of cellular and anatomic or functional continuity of living tissue. The uncontrolled wounds can lead to significant disability, amputation and increased mortality. There are considerable challenges in the wound milieu that includes hypoxia, oxidative stress, ischemia, bacterial infection, the formation of bioflim and inflammation cells at the site of injury. Understanding the mechanism that restores wound associated damage by accelerating the regeneration of healthy tissue is important to develop successful therapeutic strategies [1–5]. Biotechnological approaches based on growth factors, stem cell replacement, small-molecule drugs and RNA interference have been tried to ensure an efficient wound healing process with limited success [2,3]. Growth factors such as recombinant epidermal growth factor (EGF), vascular endothelial growth factor (VEGF), and fibroblast growth factor (FGF) have been used to stimulate wound angiogenesis, matrix deposition and re-epithelialization [2–6]. The report emphasizes that the growth factors and their receptors regulate key aspects of wound healing. Macrophages and monocytes support wound angiogenesis by releasing angiogenic factors such as VEGF, Ang-1, platelet derived growth factors (PDGF), Transforming growth factor α (TGF-α), FGF, interleukin-8 (IL-8), and tumor necrosis factor alpha (TNF-α) in wound milieu [3]. Results of clinical investigations reviewed that the treatment of growth factors accelerates healing of impaired wounds [4]. Poor outcome of single growth factor treatment of wound possibly attributes to shorter half-life of growth factor due to protease activity and poor delivery mechanisms.

Indigenously produced gasotransmitters such as NO, CO, and H_2S are equally important factors like growth factors in the process of wound healing. Depending upon the types of gasotransmitter, the signaling mechanisms can stimulate upregulation of FGF2, VEGF, activation of matrix metalloproteinases (MMPs), stimulation of Phosphoinositide 3-kinase (PI3K), upregulation of tissue inhibitors of matrix metalloproteinases (TIMPs) and activation of the inducible

* Corresponding author. AU-KBC Research Centre, M.I.T Campus of Anna University, Chromepet, Chennai 600044, India.
E-mail addresses: vimalr50@gmail.com (S. Vimalraj), soovro@yahoo.ca (S. Chatterjee).

https://doi.org/10.1016/j.niox.2018.11.001
Received 5 March 2018; Received in revised form 19 September 2018; Accepted 7 November 2018
Available online 12 November 2018
1089-8603/

isoform of cyclooxygenase (COX2) [5]. The significant amount of work has been directed to explore NO role in wound healing [14]. Since NO is a candidate which simultaneously promotes epithelialization and neovascularization and it is an obvious target for developing a wound healing strategy. Therefore, unraveling the exact role of NO in wound healing in the perspective of neo-vascularization is critical for developing the therapeutic strategy. The induced NO produced in the early phase of wound repair by inflammatory cells, mostly by macrophages [10–23]. However, it is evident that various types of cells in wound milieu are involved in producing NO during the healing process [5,6]. The work of Witte and Barbul (2002) demonstrated that the NO synthesized by iNOS promotes collagen deposition, cell proliferation and wound contraction during wound repair [23]. The positive role of NO in wound repair possibly ensured by regulating inflammation, cell proliferation, angiogenesis, matrix deposition and remodeling in the healing process [7]. NO regulates critically endothelial cells for its survival, protection against apoptosis, and promotes endothelial cell proliferation and differentiation [21–23]. The molecular mechanisms of endothelial remodeling have been studied in depth for the last 20 years [2–6]. However, the NO implications in wound angiogenesis, and mechanistic insight of the events have not been explored yet. We hypothesize that NO regulates the patterns of angiogenesis in wound milieu to optimize the healing process. The intussusceptive angiogenesis (IA), an alternative option of angiogenesis based on the longitudinal splitting of blood vessels, directs the patterning of vascular bed and perfusion. We postulate that a delicate and dynamic balance of IA and sprouting directs the healing process; and NO plays defining the role in this process. Hence, the current study focuses on NO control over the pattern of wound angiogenesis that places sprouting and IA angiogenesis in a delicate balance in repairing milieu. Further, the work critically compares re-generation and healing processes using three models; chick embryo extra-vasculature (CEV) wound, adult zebrafish skin wound, and Tie2-GFP transgenic Zebrafish caudal fin regeneration.

2. Materials and methods

2.1. Ex-ovo CEV burn wound model development

Pre-incubated white Leghorn chick (*Gallus domesticus L.*) eggs were purchased from the Government Poultry Station, Potheri in Chennai. Eggs were incubated in the Southern Humidified Incubator; temperature and humidity were maintained at 37 °C and 60%, respectively. All experiments were performed on 4th day embryos. The shell is cut open and the embryo with intact area vasculosa is carefully transferred to a Petri dish/foam cups and incubated in a sterile incubator 1 to 2 more days. Blood vessel formation becomes apparent by this time and thus we can use that system for our specific studies. 1 mm^2 area of burn wounds was made on CEV with the aid of a pre-heated surgical needle under a stereomicroscope (Olympus, India) equipped with Magnus, microscope digital camera. A size # 6 surgical needle was heated on the blue flame till red hot and used it for burn wound in CEV. The same size # 6 surgical needle was used to generate mechanical wound in CEV. The entire study was performed with burn wound model. The wounds were treated with L-nitro-L-arginine-methyl ester (L-NAME; 1 mM (NOS inhibitor), Spermine NONOate (SPNO) (NO donor); 10 mM, Sodium Nitrite, $NaNO_2$ (0.43 mM), Sodium nitrate, $NaNO_3$ (0.35 mM), phosphate buffer saline (BPS) as a control and positive control (povidone-iodine, BetaRite ointment). $NaNO_2$ and $NaNO_3$ concentrations were fixed based on previous literature that they have used it for different treatments [6,8,14]. The beetroot powder contains 79.04 μg/g nitrite and 16478.07 μg/g of nitrate [9]. Beetroot juice was prepared by fine grinding and sugar present in the juice was partially removed by acetone precipitation. The solvent was removed by rotary evaporator and tried it in 60^{O}C for 6 h to prepare a powder form; it termed as beetroot juice without sugar (BJS(−)). Beetroot juice with sugar (BJS (+)) is without acetone precipitation. BJS (−) and BJS (+) (5%W/V) dissolved in PBS and used for treatment. A specific volume of the NO donor/inhibitor was taken in the micro glass pipette and injected into the desired blood vessel using micro-injector under a stereomicroscope. After injection, micropipette was taken out very slowly to avoid any serious injury to the blood vessel. Another set of experiments was prepared with NO donors/inhibitor in a paper patch where egg yolks were incubated with 500 μmol solutions on a filter paper disc for 6hrs. After the injection/patching the embryo was incubated at 37 °C and specific humidity. During this incubation period, blood vessel formation was tracked under a stereomicroscope and micro videograph was also taken. The vascular beds were examined by injecting FITC under an intravital fluorescence microscope. Significant difference of growth pattern between control and NO donors/inhibitor was examined. The early phase of treatment (the zero minute treatment) was initiated just after the wound created, and the late phase of treatment was carried out after 30 min of the wound created. These images were analyzed using AngioQuant software [10,15].

2.2. Caudal fin regeneration assay using Tie2-GFP transgenic Zebrafish

The Tg(Tie2:EGFP)^{s849} Zebrafish line was purchased from the Zebrafish International Resource Center. The procedure was carried out as described elsewhere [14]. 10–14 months old Tg(Tie2:EGFP)s849 Zebrafish was subjected to the experiment and it was maintained under 14 h/10 h day-night cycle with 30 °C temperature condition. An automated stereomicroscope (Leica Microsystems M205FA) with equipped Canon EOS 5D Mark II camera was used. The caudal fin amputation (~50% lesion size) was made using a razor blade and the treatment was carried out on target site. The fish was anesthetized using 0.13% Tricaine (w/v), before subjecting to amputations and during the observation.

2.3. In vivo Zebrafish wound model

Adult zebrafish (*Danio rerio*) were mechanically injured by a surgical scalpel at the age of 8–10 months as described elsewhere [11]. The fish was anesthetized in 0.13% Tricaine (w/v), and a full thickness wound (~2 mm in diameter) was made in the flank region directly anterior of the anal and dorsal fins. Methylene blue staining was performed in wound area to confirm the uniformity of the diameter and depth, and it was measured by ImageJ software. The treatment was carried out by target mode at the site of the wound. The wound area was treated with L-NAME; 1 mM (NOS inhibitor), SPNO (NO donor); 10 mM, $NaNO_2$ (0.43 mM), $NaNO_3$ (0.35 mM), phosphate buffer saline (control) and positive control (povidone-iodine, BetaRite ointment). The early phase of treatment (the zero minute treatment) was initiated just after the wound created, and the late phase of treatment was carried out after 2 h of the wound created. After treatment, the fishes were kept alive for next 20 min by providing a minimal supply of water to the anterior part of fish before introducing into the water system.

2.4. Histological analysis

Adult fish were fixed in 4% paraformaldehyde in PBS overnight. It was processed and embedded in paraffin wax followed by 5 μm of sections were made in transversely. The sections were stained with Haematoxylin and Eosin (H&E) to examine the morphology of cells and tissues of the wound area and also stained with Masson's Trichrome (MT) to examine the collagen deposition in the wound area. The images were captured in the inverted microscope and analyzed by pathologists. The collagen density was evaluated based on the measurement of blue color intensity which represents the deposited collagen density. The obtained images were subjected into ImageJ software to quantify the blue color intensity in the wound area. The relative measurement of deposited collagen density was compared between treated and control wound area at 40 × magnification. The procedures were followed as

described previously [16,17].

2.5. Real time RT-PCR

At the end of treatment, the wound area from CEV and Zebrafish was excised, and total RNA was isolated from the tissue cells with Trizol reagent (Invitrogen) according to the manufacturer's instructions. The total isolated RNA was quantified with Nanodrop 2000 spectrophotometer (Thermo Scientific). cDNA was synthesized using Reverse Transcriptase kit according to the manufacturer's protocol (Invitrogen, CA, USA). The real-time PCR analysis was performed using a KAPA SYBR FAST qPCR Kit (Kapa biosystem, MA, USA). mRNA primers and internal control, β-actin primers used for amplification are shown in Supplementary Table 1. The thermal cycling profile was as follows: 95^{O}C for 5 min as initial denaturation, followed by 40 cycles of 95^{O}C for 30s, 58^{O}C for 30 s and 72^{O}Cfor 30s, with a final extension at 72^{O}C for 5 min. The relative mRNA expression was calculated by using the delta delta Ct method as described elsewhere [18–20].

(Supplementary Table 1)

2.6. Statistical analysis

All data were presented as mean ± standard deviation based on at least three replicates for each treatment. The significant difference ($p < 0.05$) between groups was determined by the Student's t-test.

3. Results

3.1. Development of Ex-ovo CEV burn wound model

The chick egg model utilized in the current study is an excellent model to investigate the pattern of angiogenesis in wound repair and the architecture of wound closure in post burn wound. The burn wound was created in the area vasculosa of shell-less chick embryo model using a needle mentioned in materials and method, the area where the wound is to be created was placed under the stereomicroscope, the area should be such that the wound shouldn't be inflicted on the main blood vessels, hence, the area of the plexus of tertiary capillaries was targeted and the needle is inserted roughly few millimeters into the area selected and gently withdrawn back. The procedure was illustrated as stepwise in Supplementary Fig. 1A. Additionally, the schematic diagram of longitudinal and transverse section wound in CEV is illustrated in Supplementary Fig. 1 B and C. The transverse section is matched with the experimentally obtained CEV wound image (Supplementary Fig. 1C). Initially, the mechanical-trauma was compared with burn wound and it showed that the vascular and hemodynamic response to wound depends on the nature of the wounds. Mechanical wound allows the system to drain away the blood in mushroom cloud fashion without any immediate blood congestion in the local wound area, while burn wound induces acute congestion of blood at the wound site, and drainage of blood is limited (Fig. 1A and B). Then, the vascular behavior in wounds in seconds scale dynamics was documented. The second scale dynamics vascular re-arrangements of burn wound healing has been captured by FITC fluorescence imaging in live in vivo imaging techniques. Results demonstrate that higher vascular flow and draining out of blood in the focal wound area happens within seconds of the wound created (Fig. 2A). However, a rapid cleansing of congested blood is observed within 5 min (Fig. 2B). We observed that drained away vessels lost blood while a new perfusing vessels coming into action at the 5th minute (Fig. 2C). The results suggest that the vascular and hemodynamic response to wound depends on the age of wound and nature of the wounds.

In this model, without any treatment, we have followed the time-course of the wound repair process of an experimentally induced burn wound in the chick embryo CEV. In 80% of the cases, a 1 mm^2 resection area forms a complete scar in 72hrs later. The wound was treated with commercially available povidone-iodine 5 %w/w as a positive control and allowed to heal, the observation of the wound closure (arrow mark) was done every 2 h and followed up to 6 h (Fig. 3). The scar itself consists of a granulation tissue formed by newly-formed vessels, fibroblasts and inflammatory infiltrate essentially composed of macrophages. The process of wound repair depends upon a variety of interactions between cells and the extracellular matrix components and wound repair is in part mediated by multiple growth factors released by inflammatory cells and from their storage sites of the extracellular matrix [21,22].

(Supplementary Figs. 1A–C)

3.2. Early effects of NO donor and NOS inhibitor in wound repair using CEV model

This ex-ovo model improved the access to intra-vital imaging, local treatment and tissue manipulations. The burn wounds were inflicted in the 4th day chick embryos using a heated needle and treated with respective drugs. We investigated the effect of L-NAME, a selective inhibitor of NOS and SPNO (NO donor) on wound healing pattern and microcirculation. The embryos were maintained in a horizontal egg incubator (37 °C temperature and 90% humidity) and images of the embryo were taken periodically up to 6 h. Initially, the concentrations of SPNO and L-NAME were standardized by studying their effect at different range. The vascular and hemodynamic response to the wound is depending on the age of wound (Fig. 2). Hence, to study the role of NO on wound repair mechanism through SA and IA, NO donor and NOS inhibitor treatment were carried out on CEV burn wounds, as soon as the burn wound generated and is termed as early treatment. This initial treatment showed that NO donor significantly increased the healing of wounds in CEV compared to control group. Interestingly, rapid but erroneous wound healing was observed during the removal of enzyme-dependent NO by L-NAME when compared to control and SPNO (Fig. 4). From this data, we infer that higher rate of wound healing may be due to IA which must be confirmed in further investigations. Further studies using this model will aid in discovering an effective and accelerated approach in treating burn wounds.

3.3. Angiogenic regulation of NO in early wound repair using CEV model

The adequate supply of nutrition, oxygen and other necessary micro and macromolecules to the site of injury is required through blood vessel for the healing of the wound. Hence, understanding the mechanism of vessels formation by angiogenesis is essential for various physiological and pathological phenomena. The wound angiogenesis denotes a typical model to study molecular mechanisms which belong to vascular formation and remodeling. Additionally, these angiogenesis mechanisms may offer potential therapeutic options to regulate not only wound healing but also other complications such as cancer, chronic inflammatory disorders, cardiovascular diseases, diabetic retinopathy and excessive tissue defects [21].

In the current study, we mainly focused on NO regulation of angiogenesis in wound healing. Specifically, whether NO prefers IA or SA during the wound healing process. Initially, we have selected a list of SA-like and IA-like specific marker genes based on previous literature since there is no specific marker available till now. Tumor Endothelium Marker 8 (TEM8), Caldesmon 1 (CALD1) and CXC motif chemokine receptor 4 (CXCR4) are IA-like marker genes. Tyrosine kinase with immunoglobulin-like and EGF-like domains 1 (Tie2) and Ephrin B2 are SA-like marker genes. It has been reported that TEM8 is expressed at low levels at early stages of chick CAM development and after 12 days, the mature stage of CAM the expression of TEM8 is transiently increased, the expression peak is laid between days 10 and 12 [25]. Notch inhibition promotes IA by down regulating Notch2, EphrinB2, EphrinB4, Tie2 and Hes5 genes and up regulating Cxcr4, SDF-1, FGF2

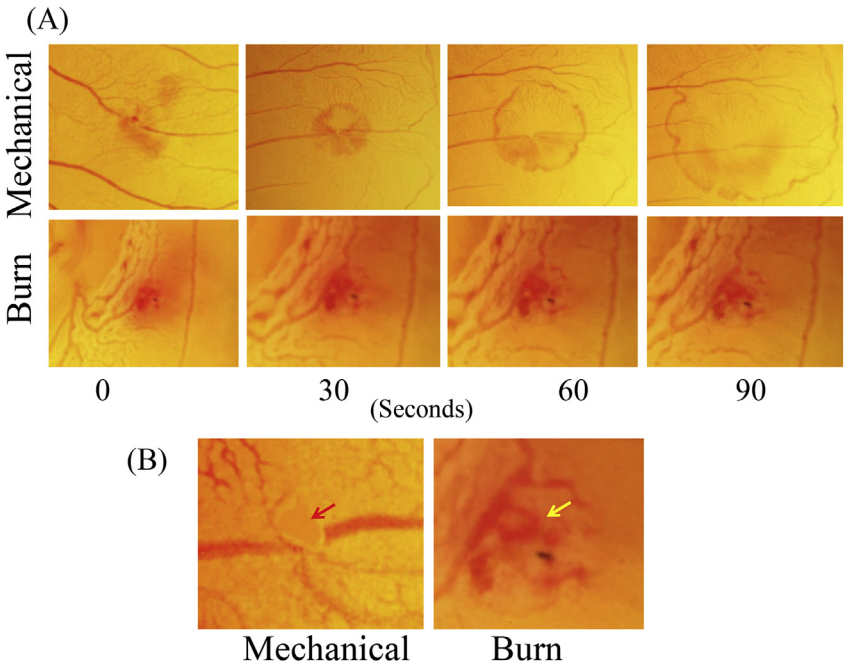

Fig. 1. Vascular and hemodynamics analyses in mechanical-trauma and burn wound in CEV. Burn wound and the mechanical wound was generated in the fourth day incubated eggs. (**A**) The images were taken every 30 s interval up to 90 s under the stereomicroscope using a digital camera. (**B**) Comparison of mechanical-trauma and burn wound in CEV.

genes [26,27]. The comparison CALD1 expression between normal blood vessels and tumor vasculature showed that it is specific to tumor vasculature. Moreover, it has been discussed that CALD1 could be an IA marker since the tumor prefers IA [28,29]. The selected marker genes expression was analyzed during chick embryo chorioallantoic membrane (CAM) development to identify their specificity [10].

During development of chick embryo, the CAM vascularization undergoes three major phases for angiogenesis. Day 5–7 is considered as an early phase (phase 1). In this phase, the system prefers for capillary network growth, and it is SA. Day 8–12 is considered as an intermediate phase (phase 2). In this phase, no longer SA, SA is replaced with IA, and at day 11 showed more frequency. Day 13–14 is considered as late phase (phase 3). In this phase, SA is more by increasing growing pillar size [30]. IA reorganizes the existing cells without proliferation, one of the important characteristic features of IA. The proliferation rate of endothelial cells was measured in CAM from day 6 to day15. The result showed that more than 50% of proliferative activity is decreased at day 10 compared to day 6, and the proliferative activity of day 14 is increased 10% compared to day 6 [31]. Based on this evidence, we have analyzed the expression of selected marker genes by real time RT-PCR analysis from day 5 to day14 of CAM development (data not shown). The result showed that Tie2 and Ephrin B2 mRNAs were increased in phase 1 (day 6 and 7), decreased in phase 2 (day 8–12), and again started to elevate at phase 3 (day 13 and 14). Hence, Tie2 and Ephrin B2 may be considered as SA-like marker genes. Similarly, IA specific genes, TEM8, CALD1, and CXCR4 are increased in phase 2 (day 8–12) compared to phase 1 and 3. Hence, these genes may be considered as IA-like marker genes.

With these backgrounds, to identify the NO regulation in wound healing in early treatment through activation of SA and/or IA we

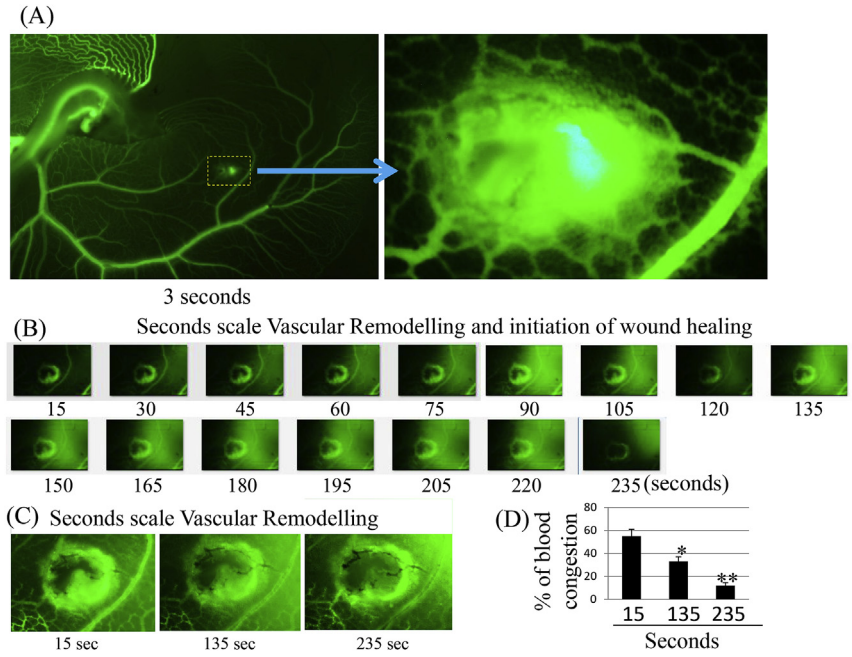

Fig. 2. Seconds scale dynamics of vascular behavior in burn wound. Burn wound was generated in the fourth day incubated eggs and the vascular beds were examined by injecting FITC under an intravital fluorescence microscope. (**A**) Hemodynamics of burn wound in 3 s (**B**) 15–235 s scale dynamics of vascular Remodeling. (**C**) Comparison of 15, 135 and 235 s vascular dynamics. (**D**) Percentage of blood congestion was calculated by ImageJ software. (*) indicates significant decrease compared to 15 s and (**) indicates significant decrease compared to 15 s and 135 s.

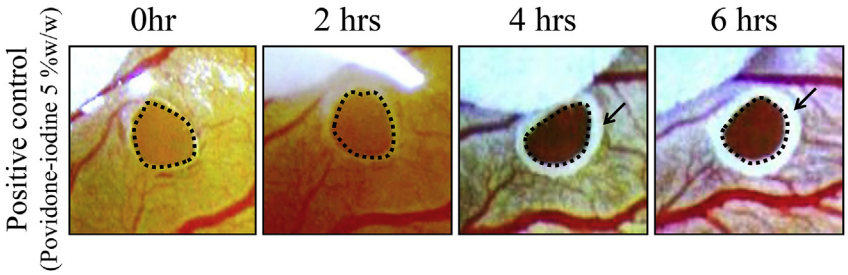

Fig. 3. A representative image of CEV wound healing model. Burn wound was created in the fourth day incubated eggs and treated with Povidone-iodine 5 %w/w as a positive control. The eggs were incubated at 37°C and 90% humidity till 6 h to show the wound closure in CEV. The images were taken at every 2 h interval up to 6 h under the stereo microscope using a digital camera. The arrow mark indicates the progression of wound closure.

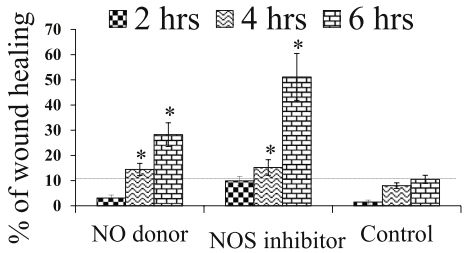

Fig. 4. NO donor and NOS inhibitor promote wound healing in the early treatment of CEV burn wound. Burn wound was created in the fourth day incubated eggs, and the treatment was carried out at an early phase of the wound (0 min). A vascular bed and heart are clearly visible in 0–6 h of L-NAME (1 mM), SPNO (10 mM) and phosphate buffer saline (control) treatment. The eggs were incubated at 37°C and 90% humidity till 6 h to study the wound healing. The vascular bed and wound closure area was calculated by ImageJ software.

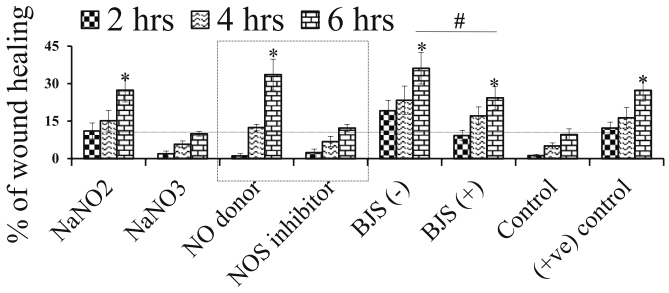

Fig. 6. NO donor promotes wound healing in the late treatment of CEV wound. The burn wound was created in CEV and treated with NO donor and NOS inhibitor at the late phase (after 30 min) of the wound, and then the eggs were incubated upto 6 h. A vascular bed and heart are clearly visible in 0–6 h of L-NAME (1 mM), SPNO (10 mM), NaNO2 (0.43 mM), NaNO3 (0.35 mM), BSJ + (5%W/V), BSJ- (5%W/V), PBS (control) and a positive control, BetaRite, commercially available ointment treatment. The eggs were incubated at 37°C and 90% humidity till 6 h to show the healing. The above-healed area was calculated by ImageJ software and plotted the graph.

analyzed above genes expression by real time RT-PCR. 6 hrs after treatment, the wound area was excised and subjected to mRNAs studies. The result showed that TEM8, CALD1 and CXCR4 were increased in NOS inhibitor treatment compared to control and NO donor treated wound (Fig. 5) whereas Tie2 and Ephrin B2 were increased in NO donor treatment compared to NOS inhibitor and control wound (Fig. 5). Previously, Fig. 4 showed that both NO donor and NOS inhibitor were involved in the promotion of wound healing process. The results from Figs. 4 and 5 suggest that NO donor promotes wound healing through SA and NOS inhibitor promotes wound healing through IA in early treatment of CEV burn wound.

3.4. Late effects of NO donor and NOS inhibitor in wound repair using CEV model

Figs. 4 and 5 showed that both NO donor and NOS inhibitor promote wound healing, but with a different angiogenic mechanism. Further, we analyzed whether the same mechanism occurs in the late wound treatment as well (30 min after wounding). iNOS expression is measured in human burn wound; the result showed that iNOS expression is high in immediately after wounding. Different cells in and around the wound showed different levels of iNOS expression [32,33].

It was suggested that iNOS might play a role in initial inflammatory response to burn wound [33]. When the age of the wound has increased the expression of iNOS is decreased due to proliferated and migrated cells resurfaced the epidermal edges [34]. This evidence showed that the NO level is varies based on the age of the wound. Hence, to understand the NO regulation in wound healing after 30 min of wounding we treated the CEV burn wound with and without NO donor and NOS inhibitor along with control and positive control (Fig. 6). Initially, it is treated with the different time period of post wounding to determined late phase of treatment upto 4 h. After 30 min to 4 h of treatment showed similar pattern of wound healing with NO donor and NOS inhibitor treatment. The treatment of NO donor and NOS inhibitor after 30 min of wound showed that NO donor increased the percentage of wound healing compared to control and NOS inhibitor. Interestingly, NO inhibitor is not increased wound healing process significantly. This result is completely reversed from the early treatment of NOS inhibitor in CEV burn wound (Fig. 4). This result suggests that NO regulation in wound healing depends on the availability of systemic NO level.

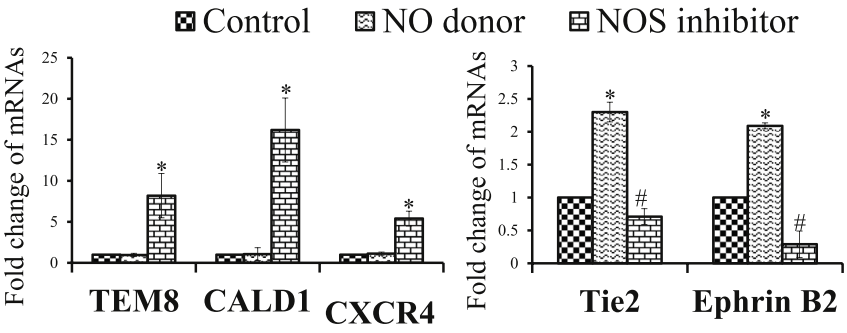

Fig. 5. NOS inhibitor promotes wound healing through IA, and NO donor promotes wound healing through SA in early treatment of CEV model. The burn wound was generated in CEV and treated with NO donor and NOS inhibitor at an early phase of the wound, and then the eggs were incubated up to 6 h. The wound area in CEV was excised and subjected to RNA isolation followed by real time PCR analysis for the TEM8, CALD1, CXCR4, Tie2 and Ephrin B2 mRNAs expression. IA-like marker genes, TEM8, CALD1 and CXCR4 (left panel) and SA-like marker genes, Tie2 and Ephrin B2 (right panel). Fold change of these mRNAs was calculated after normalization with β-actin mRNAs. (*) indicates significant up regulation of mRNA compared to control wound and NO donor treatment. (#) indicates significant down regulation compared to control and NOdonor.

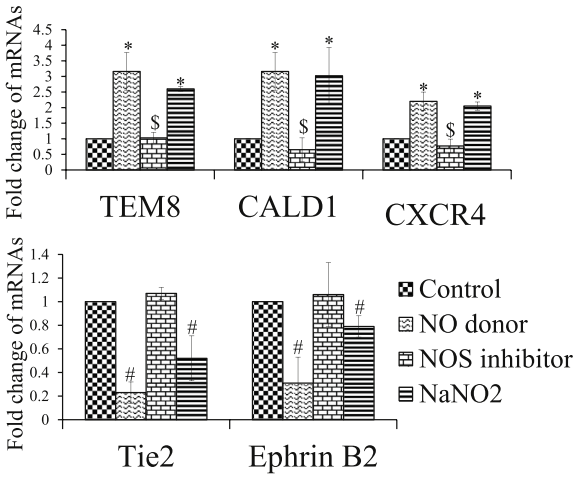

Fig. 7. NO donor increases wound healing through IA in the late treatment of CEV wound. The burn wound was created in CEV and treated with L- NAME (1 mM), SPNO (10 mM) and NaNO2 (0.43 mM) along with PBS after 30 min of wounding in CAM. The eggs were then incubated upto 6 h. The wound area in CEV was excised and subjected to RNA isolation followed by real time PCR was carried out using the primers for TEM8, CALD1, CXCR4, Tie2 and Ephrin B2 gene. IA-like marker genes, TEM8, CALD1 and CXCR4 (upper panel) and SA-like marker genes, Tie2 and Ephrin B2 (lower panel). Fold change of these mRNAs was calculated after normalization with β-actin mRNAs. (*) indicates significant up and (#) indicates significant downregulation of mRNA compared to control and NO donor treatment group. ($) indicates significant down regulation compared to NO donor treatment.

3.5. Angiogenic regulation of NO in late wound repair using CEV model

Burn wound was generated in CEV model and after 30 min of wounding it was treated with NO donor and NOS inhibitor as described in materials and methods. To understand NO regulation in wound healing at late treatment through activation of SA or IA we analyzed mRNAs expression of TEM8, CALD1, CXCR4, Tie2 and Ephrin B2 by real time RT-PCR. 6 hrs after treatment, the wound area was excised and subjected to mRNAs studies. The result showed that TEM8, CALD1 and CXCR4 were increased in NO donor treatment compared to control and NOS inhibitor treated wound (Fig. 7), and Tie2 and Ephrin B2 were decreased in NO donor treatment compared to NOS inhibitor and control wound (Fig. 7). Fig. 6 showed that NO donor promotes wound healing process. These results suggest that NO donor promotes wound healing through increasing IA and decreasing SA in the late treatment of CEV burn wound.

3.6. Effects of $NaNO_2$, $NaNO_3$, BSJ (+) and BJS (−) on wound healing using CEV model

To further analysis the nitrite and nitrate influence on wound healing, we used $NaNO_2$ (43 mM) and $NaNO_3$ (0.35 mM) in CEV burn wound model. Treatment was carried out after 30 min of wounding. The result showed that NaNO2 significantly increase the wound healing compared to control, whereas $NaNO_3$ showed no significant change in healing progress (Fig. 6). These results correlate with previous literature [32–36]. Additionally, to understand the $NaNO_2$ regulation of angiogenesis in wound healing process we generated burn wound in CEV and after 30 min $NaNO_2$ treatment was carried out and followed by real time RT-PCR analysis was performed for SA and IA markers expression. The result showed that $NaNO_2$ promotes wound healing by upregulating IA and downregulating SA in late burn wound (Fig. 7). Additionally, BSJ(+) and BSJ(−) were treated with CEV burn wound to assess their ability to check in wound healing properties since the beetroot possesses a rich nitrate, nitrite and other phytochemicals [35]. Both BSJ(+) and BSJ(−) is significantly increased wound healing compared to control wound whereas there was no significant difference between BSJ(+) and BSJ(−) treatment (Fig. 6). These results showed that NaNO2, BSJ(+) and BSJ(−) are an effective in improving wound healing process. Initially, we used these molecules to evaluate the developed CEV burn wound healing model. It showed a strong progression on the healing process. Hence, we continued other treatment with this developed CEV burn wound model. However, it further warrants detailed studies on these molecules to confirm on the wound healing process. These molecules may use in clinically in means of topically delivering of NO to augment wound healing, and this may have clinical benefits.

3.7. Early effects of NO in wound repair using caudal fin regeneration assay using Tie2-GFP transgenic Zebrafish

To study the implications of NO on wound healing and wound angiogenesis in an embryonic model we used chicken CEV burn wound model (Fig. 4). To further evaluate the NO regulation in wound healing and wound angiogenesis in adult we used Zebrafish caudal fin regeneration assay and skin wound model. In order to investigate NO implication in regeneration and angiogenesis the adult Tie2-GFP transgenic Zebrafish caudal fin regeneration assay was used. Half of the fin was amputated for each adult Tie2-GFP Zebrafish using a sterile razor blade and treated with either in 0.001% 1xPBS or 5 mM NO donor (SPNO) or 5 mM NO inhibitor (L-NAME) for 20 min and then the fishes were placed back to their tanks. Bright field and fluorescent images of the regeneration of the fin after 48 h of 1xPBS or NO donor or NO inhibitor treatment were taken (Fig. 8). The result showed that the cute fins of the NO donor or NO inhibitor treated Tie2-GFP Zebrafish grew faster compared to the fin of the control Tie2-GFP Zebrafish. Additionally, there were differential effects of NO stimulation and NO inhibition upon blood vessel re-growth during the regeneration of the fin. NO donor treatment induced increased SA while NO inhibitor treatment induced pillar formation in the regeneration of the fin. Pillar formation is a morphological feature of IA.

3.8. Early and late effects of NO in wound repair using Zebrafish skin wound model

Zebrafish skin wound model has been adapted from previously described literature [11,12]. In embryogenesis wound healing model is rapid and scar-free, whereas in adult wound healing model it processed by several steps that are (1) blood clotting, (2) inflammation, (3) re-epithelialization, (4) vascularization, (5) granulated tissue formation (6) maturation and (7) scar formation. Adult Zebrafish skin wound model is following all the steps in the mammalian wound model except the formation of external fibrin clots. Furthermore, the Zebrafish skin wound model has certain advantages such as it shows extremely rapid re-epithelial cell formation at the site of the wound without lag phase. This process pre-porn the other wound healing mechanism such as inflammatory cell migration, vascularization, granulation tissue formation, accumulation of macrophages, fibroblasts, blood vessels and collagen deposition compared to the mammalian wound model [11,12]. Zebrafish is well known model for angiogenesis research [37].

In particular, repair of skin defects offers an ideal model to analyze angiogenesis due to its easy accessibility to control and manipulate this process. Most of those growth factors, extracellular matrix molecules, and cell types, recently discovered and considered as crucial factors in blood vessel formation, have been identified and analyzed during skin repair and the process of wound angiogenesis [2,38]. We have also used Adult Zebrafish as a model to study angiogenesis in tissue regeneration (unpublished data). Hence, to identify NO regulation in wound repair and wound healing angiogenesis whether SA or IA we generated skin wound in the flank region of Zebrafish and administrated with NO donor, NOS inhibitor, $NaNO_2$, control and positive control as described in materials and method. The treatment was carried out in 0 min of post

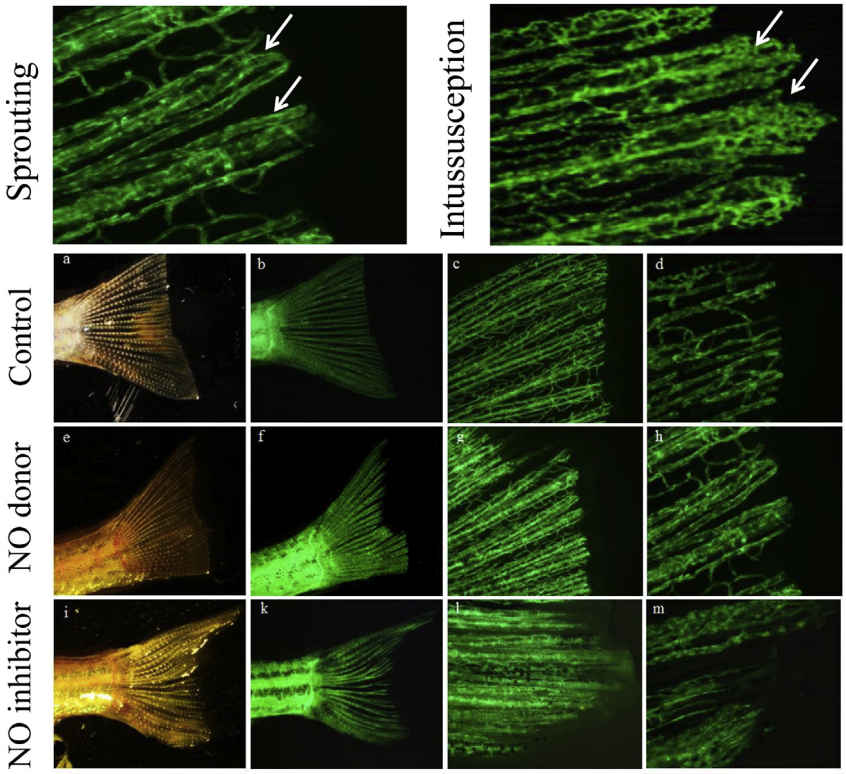

Fig. 8. The effects of NO stimulation or inhibition upon the regeneration and angiogenesis of the adult Tie2-GFP transgenic zebrafish tail fin after 48 h of treatment (a–m). Half of the fin was amputated for each adult Tie2-GFP zebrafish using a sterile razor blade. Brightfield (a, e, i) and fluorescent images (b-d, f-h, k-m) of the cut and uncut fins at different magnifications were taken. After cutting half of the fin, the Tie2-GFP zebrafishes were placed either in 0.001% 1xPBS or 5 mM NO donor (SPNO) or 5 mM NO inhibitor (L-NAME) for 20 min and then the fishes were placed back to their tanks. The images show that the cutted fins of the NO donor or NO inhibitor treated Tie2-GFP zebrafish grew faster compared to the fin of the control Tie2-GFP zebrafish. Additionally, there were differential effects of NO stimulation vs. NO inhibition upon blood vessel re-growth during the regeneration of the fin. NO donor treatment induced increased SA (g, h) while NO inhibitor treatment induced pillar formation in the regeneration of the fin (l, m). Upper panels are representative images of SA and IA. Magnification 10X: (a,b, e, f, i, k), 52X: (c, g, l), and 160X: (d, h, m).

wounding (early phase of treatment) and 1 h of post wounding (late phase of treatment). After 24 h of treatment, the wound area was subjected to histological analysis to understand re-epithelization and granulation by H&E staining. And, after 48 h of treatment, the wound area was subjected to histological analysis to examine the collagen deposition by Masson's Trichrome staining. Initially, the generated wounds have lost their all dermal and epidermal-dermal cells, scales and subcutaneous adipocytes, whereas the primary muscle tissues are not damaged. This was confirmed by methylene blue dye penetration assay and H&E staining of control tissues (Fig. 9A, a,b). At 24hrs, the treatment of NO donor, NOS inhibitor, and $NaNO_2$ after 0 min of wounding showed that the wound is completely granulated with multiple cell layers. The granulated cell layer is indicated by an arrow mark (Fig. 9A c,d,e). Additionally, NOS inhibitor showed more granulated cells compared to NO donor, and $NaNO_2$ treated wounds. When the same treatment was given after 1 h of wounding the result of NOS inhibitor showed less/no granulation whereas NO donor and $NaNO_2$ showed complete granulated cells at the wound site (Fig. 9A, f,g,h). Specifically, NO donor and NaNO2 showed granulated cells at both early and late treatment of wound whereas NOS inhibitor showed high granulated cells at early treatment and less/no granulated cells at late treatment (Fig. 9A, d,g).

This result suggests that NO donor enhance the wound healing process both in early and late treatment, whereas NOS inhibitor enhances wound healing only at early treatment. In mammalian wound repair mechanisms, the inflammation and re-epithelialization are overlapping with the formation of tissue granulation, which is characterized by the accumulation of fibroblastic cells, macrophages, and new blood vessels into the wound site beneath the neoepidermis [3,39]. In normal wound healing in the Zebrafish skin without any treatment, the granulated tissues can be identified at 2 days of post wound [11] whereas the treatment can pre-porn the tissue granulation.

On the surface of the wound, epidermal cells burst into mitotic activity within 24–72 h. These cells start their migration across the wound surface. The fibroblast proliferates in the deeper parts of the wound. This fibroblast begins to synthesize small amounts of collagen, which acts as a scaffold for migration and further fibroblast proliferation. Granulation tissue, which is made up of capillary loops, supported in this collagen matrix formation, also occurs in the bottom layers of the wound. The proliferation phase lasts from 24 to 72 h and leads to the fibroblastic phase of wound healing [4,40]. Collagen deposition in wound healing is an important characteristic feature to identify the healing process. Moreover, it facilitates to regain of the damaged tissues, where it reestablishes the original function and structure of tissues [4,40].

Hence, to identify the collagen deposition the Masson's Trichrome staining was performed in Zebrafish skin wound histology sections (Fig. 9B). The stained sections were subjected to ImageJ analysis to get the quantitative measurements of collagen deposition (Fig. 9C). This quantitative analysis helps for comparison studies. At 48 h, the treatment of NO donor, NOS inhibitor, and $NaNO_2$ after 0 min of wounding showed that a thick layer collagen was deposited in the wound area. A blue cell layer of collagen deposition is indicated by an arrow mark (Fig. 9B c',d',e' and 6C). Additionally, NOS inhibitor showed more collagen deposition compared to NO donor, and NaNO2 treated wounds (Fig. 9B c',d',e' and 6C). When the same treatment was given after 1 h of wounding the result of NOS inhibitor showed less collagen deposition whereas NO donor and $NaNO_2$ showed significant levels of collagen deposition (Fig. 9B, f ',g',h', 6C). Specifically, NO donor and NaNO2 showed collagen deposition at both early and late treatment of wound whereas NOS inhibitor showed high collagen deposition at early treatment and showed significantly reduced collagen deposition at late treatment (Fig. 9B, d,g, 9C). These results suggest that NO donor enhance the wound healing process both in early and late treatment, whereas NOS inhibitor enhances wound healing only at early treatment. To understand the underlying mechanism of wound repair by NO donor and NOS inhibitor through angiogenesis the following section has been analyzed SA and IA like marker genes expression during wound healing.

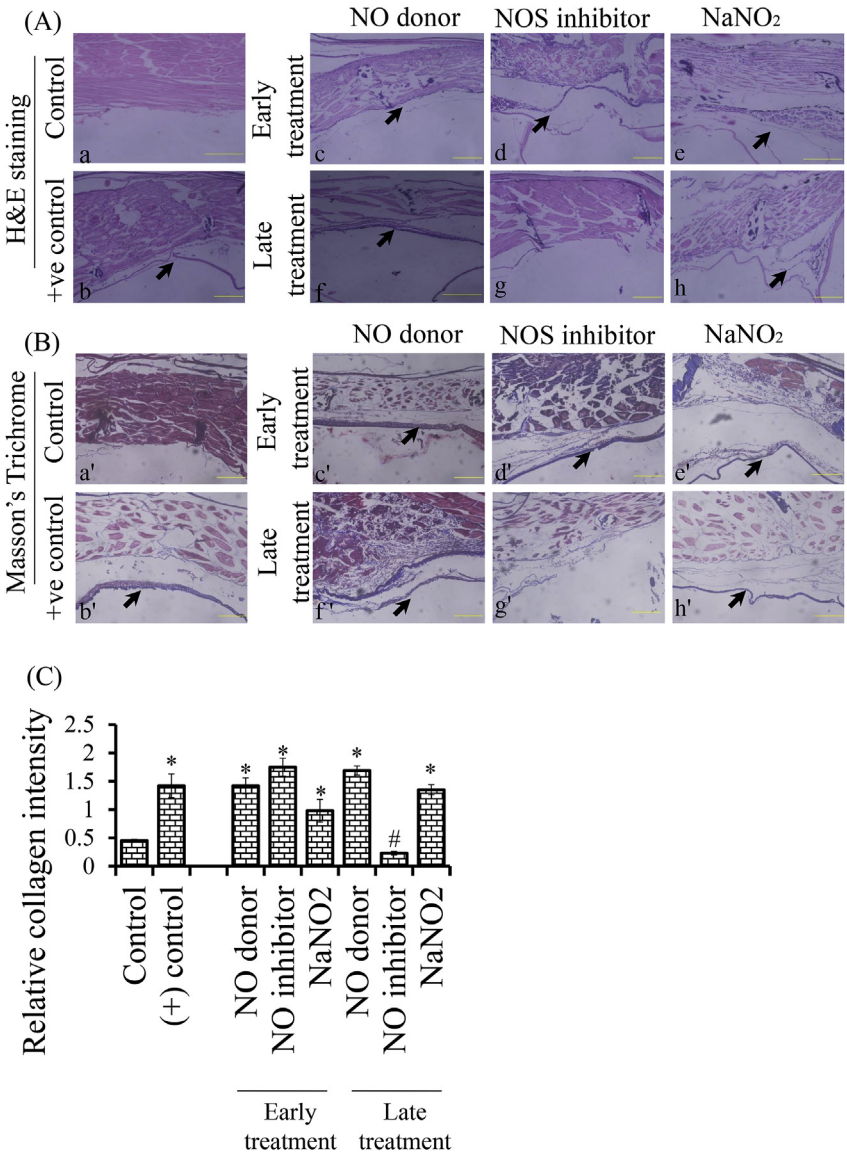

Fig. 9. NO donor increases epithelization and collagen deposition in early and late treatment, but NOS inhibitor increases epithelization and collagen deposition only in early treatment. The wound was generated in the flank of Zebrafish as described in materials and method section. The targeted treatment was carried out with L- NAME (1 mM), SPNO (10 mM) and NaNO2 (0.43 mM) along with PBS at an early phase and late phase of the wound. After 24 h, the wound was subjected to histological analysis to understand the wound healing mechanisms. (A) H&E staining of a transversal section through the wound depicts the healing process by showing the cell and tissue morphological changes in the wound area. (a) Control, (b) positive control, (c) NO donor (early phase), (d) NOS inhibitor (early phase), (e) NaNO2 (early phase), (f) NO donor (late phase), (g) NOS inhibitor (late phase), (h) NaNO2 (late phase). (**B**) Similarly, to understand collagen deposition in wound healing process under treatment the Masson's Trichrome staining was performed after 48 h of treatment. (a') Control, (b') positive control, (c') NO donor (early phase), (d') NOS inhibitor (early phase), (e') NaNO2 (early phase), (f ') NO donor (late phase), (g') NOS inhibitor (late phase), (h') NaNO2 (late phase). Scale bars are equal to50 μm for all images. (**C**) The collagen deposition of the above sections was measured by ImageJ software, and the quantitative graph was plotted.

3.9. Angiogenic regulation of NO in wound repair using Zebrafish skin wound model

The wound was generated in the flank region of adult Zebrafish and after 0 min and after 1 h of wounding it was treated with NO donor, NOS inhibitor and $NaNO_2$ as described in materials and methods. To understand NO regulation in wound healing at early and late treatment through activation of SA or IA we analyzed mRNAs expression of TEM8 and Tie2 by real time RT-PCR. 48 hrs after treatment, the wound area from Zebrafish, was excised and subjected to mRNAs studies. In early treatment, the result showed that TEM8 was increased and Tie2 was decreased in NO NOS inhibitor treatment compared to control, and NO donor treated wound whereas NO donor and NaNO2 increased Tie2 expression in early treatment (Fig. 10). The result of late treatment showed that NOS inhibitor treatment decreased TEM8 expression, whereas NO donor and NaNO2 treatment increased TEM8, and decreased Tie2 expression control wound (Fig. 10). Figs. 6 and 7 showed that both NO donor and NOS inhibitor promote wound healing process in early treatment but the different angiogenic mechanism. Specifically, NO donor prefers SA and NOS inhibitor prefer IA in early treatment. However, the late treatment showed only NO donor has the implication in the promotion of wound healing through IA angiogenesis. NO donor has wound healing property with a different angiogenic mechanism

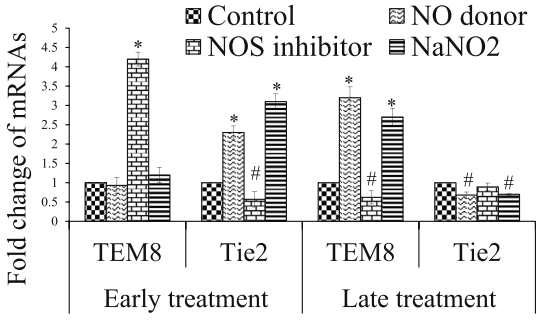

Fig. 10. NOS inhibitor increase IA and decrease SA in early treatment of wound healing, and NO donor promotes SA in early treatment and increases IA in the late treatment of wound healing. The wound was generated in Zebrafish and treated with L- NAME (1 mM), SPNO (10 mM) and $NaNO_2$ (0.43 mM) along with PBS at early and late phase of the wound. After 48 h, the wound area was excised and subjected to RNA isolation followed by real time PCR analysis was performed using the primers for TEM8, and Tie2 genes. Fold change of these mRNAs was calculated after normalization with β-actin mRNAs. (*) indicates significant up regulation of mRNA compared to control wound. (#) indicates significant down regulation compared to control wound.

based on the treatment period. The results obtained from adult Zebrafish skin wound model is supported each other with chick embryonic CEV burn wound model. Additionally, these results suggest that NO have a similar effect both in an embryonic and adult wound model.

4. Discussion

The wound healing process has been divided into four discrete temporal phases, namely coagulation, inflammation, proliferation, and remodeling. The initial coagulation phase, during the first 1–2 h of wound healing process, is dominated by the activation of platelets, coagulation and fibrin clot formation. In this process, as they degranulate, platelets release cytokines and growth factors which are essential to the wound healing process. We envisage that NO comes into action immediately after the wound created and starts defining angiogenesis process to shape the time-dependent healing events. Angiogenesis is confined to the wound site and plays a pivotal role for successful wound healing. Revascularization is required to furnish the new tissue and metabolites and to dispose of the waste products of metabolism. Angiogenesis occurs as a higher regulated process which is rapidly stimulated after injury and ceases when wound healing is complete.

To understand the mechanism of NO regulation in wound healing through angiogenesis, we used CEV burn wound model, caudal fin regeneration assay using Tie2-GFP transgenic Zebrafish and Zebrafish skin wound model. The CEV burn wound model is a novel model used in the current study (Figs. 1–3). However, CEV burn wound model does not strictly represent adult wounds since TGF-β3 is expressed in embryo only and it plays a unique anti-scar role [41,42]. It has been discussed that the neutralization of TGF-β3 promotes scar formation. CEV burn wound is as an embryonic model, while caudal fin regeneration assay using Tie2-GFP transgenic Zebrafish and Zebrafish skin wound model are adult models. In these models, NO donor and NOS inhibitor were treated in the early phase and late phase of the wound. The results showed that both NO donor and NOS inhibitor promoted wound healing compared to control, whereas the NOS inhibitor administration is further increased wound healing compared to NO donor in the early phase of treatment (Figs. 4, 8 and 9). At late phase, NO donor promotes wound healing whereas NOS inhibitor failed to promote (Figs. 6 and 9). NO donor involved in the promotion of wound healing is supported by previous reports [23,43]. Specifically, an early treatment of wound with NOS inhibitor induces wound healing by promoting IA whereas NO donor induces wound healing by activating SA (Figs. 4–10). However, a late treatment of the wounds with NO donor promotes wound healing by IA. This was confirmed by morphological and real time RT-PCR analysis of marker gene expression for SA and IA respectively (Figs. 5, 7, 8 and 10).

The literature emphasizes that the inducible nitric oxide (iNOS) is produced by inflammatory cells specifically by macrophages in the early phase of wound healing process. Additionally, other cells in the wound microenvironment also reported being involved in NO production during the proliferative phase. iNOS produced NO positively promoted cell proliferation, collagen synthesis and wound closure during wound repair. NO donor treatment increases the wound healing process in iNOS deletion animal model [23]. It has been observed that NO influences wound repair by regulating inflammation, cell proliferation, matrix deposition, angiogenesis and remodeling [44]. However, the mechanism of NOS inhibitor-associated stimulation of wound healing is not understood yet. However, the report showed that the inhibition of iNOS by L-NAME and N^5-(1-Imino-methyl)-L-ornithine (L-NIO) promotes wound healing by increasing the level of hydroxyproline and tensile strength [24]. L-NAME treatment in rat wound showed increased collagen, fibroblasts proliferation and angiogenesis compared to NO donor and control [32,33,45]. Although inflammation is an inevitable step of the healing process, excessive inflammation may delay the healing process. iNOS plays a role in initial inflammatory response to burn wound [33]. Uncontrolled inflammation can jeopardize the early healing processes such as cellular migration and proliferation [2,38]. The work of Wenezak et al. (1993) demonstrated a fall in the expression profile of iNOS when the wound ages [34,46–65]. Additionally, many anti-inflammation agents like sappanone A and handelin reported to show potential NOS inhibition effects [60–62]. Specifically, the inhibitory effect of handelin on neuroinflammation is documented by down regulation of iNOS and cyclooxygenase 2 (COX2) expressions [61]. Sappanone A decreases the releases of NO, TNF-α, Interleukin 6 (IL-6), and Prostaglandin E2 (PGE2) signaling and down regulates the expressions of iNOS, TNF-α, IL-6, IL-1β, Monocyte Chemoattractant Protein-1 (MCP-1), and COX-2 in microglial cells [62]. L-NAME, N^G-monomethyl-L-arginine (MMA), N^G, N^G-dimethyl-L-arginine (asymmetric dimethylarginine, ADMA) and N^G,N'^G-dimethyl-L-arginine (symmetric dimethylarginine, SDMA) are the inhibitors of NOS activity [63]. Nitrate/nitrite metabolism produces a mutagenic byproduct, the nitrosating agent N_2O_3 (nitrous anhydride) and during nitrate/nitrite metabolism, mutagenic reactive nitrogen oxides, such as nitrous acid (HNO_2) and NO, are formed [64]. It has been reported that IA, a primary angiogenesis mechanism of microvascular adaptation for prolonged inflammation [46], is stimulated by inflammation in murine colitis. Patan et al. (2001) elaborated the mechanisms of vascular morphogenesis in wound repair using the mouse ovariectomy model. In this model, after ovariectomy, the tissues were exposed to a non-inflammatory wound healing process as the similar healing process of surgical wounds. The system triggers IA for the healing of the ovarian pedicle which was identified based on intervascular tissue structures and loop formation and segmentation of new vessels. Additionally, it has been reported that the blind ending sprouts, SA were exceedingly rare [39]. The IA was tracked and analyzed in mouse skin wound model that showed the appearance of SA on day 5 of post-treatment but not the IA. The reason has been discussed as the lack of IA in skin wounds is due to neither pillar development nor the IA itself is an invasive process [47].

The wound angiogenesis denotes a typical model for studying molecular mechanisms which belong to vascular formation and remodeling in general. Our finding showed that NO regulates wound healing by different angiogenesis mechanisms. Metabolic stimuli and biomechanical forces generated by blood flow and its pattern play important roles in vascular development, vessel regression and vascular remodeling by differentially expression the gene pattern [48]. The hemodynamics, oxygen supply, vascular functions are very different in the abrupt wound to those of chronic wound. Therefore, we envisage that applying NO or removing NO from the wound milieu and its impacts depend on the stages of the wound as we have observed in the present study. Hypoxia, deficiency in oxygen stimulates IA in mouse retina [49], and erythropoietin induces IA [50]. It is reported that the increased wall shear stress stimulates IA in skeletal muscle [51]. The profile of biomolecule present in micro-environment of the wound is varied between early and late phase [52]. The mechanical forces of blood flow dynamic along with the biomolecules found in the microenvironment collectively decide the patterning of vascular remodeling. It has been discussed that the local hemodynamics plays an important role in IA formation [48,53–58]. Promoting IA in wound milieu specifically fresh and abrupt wound may help for rapid remedy.

We have extended our studies to another aspect of healing that is “regeneration” by using adult zebrafish fin tail (caudal) regeneration model. This study critically checked the dogma that NO differentially changes the type of neo-vascularization process; SA to IA, in the healing regime. Since regeneration of tissue in adults is also a part of healing it is quite important to understand NO implications in regeneration model. The caudal fin is composed of bones, mesenchymal tissue, blood vessels and nerves, skin tissues and following “stem cells” specifically after resection phase. Regeneration of caudal fin three occurs through three distinct regenerative stages: (1) wound healing [0–1 days after resection; (2) formation of the regeneration blastema (1–3 days after

resection), involves highly proliferative mesenchymal progenitor cells; and (3) regenerative patterning of new tissue initiating after 3 days of resection [59]. Present work plan restricted our study till 3rd day since we were keen to study the NO implication in the very early phase of regeneration model as have performed in zebrafish skin and CEV models respectively. The work of Petrie et al. (2014) demonstrated that macrophages play a critical role in defining the pattern of regenerated tissues in caudal fin of adult zebrafish by using Wnt/β-catenin as a signaling pathway that regulates the injury microenvironment, inflammatory cell migration and macrophage phenotype [59]. On the other hand, macrophages are known to produce iNOS and play important roles in various situations including healing [65]. Our model clearly demonstrated that applying NO or removing NOS derived NO from a tissue regeneration model could change the pattern of regeneration possibly by swinging the SA-IA mode of angiogenesis (Fig. 8).

We conclude that NO defines healing process by regulating angiogenesis mechanisms differentially that depend on the temporal dynamics of the wound. The wound repair mechanisms in CEV and adult Zebrafish skin would model would be a suitable model for studying the angiogenic mechanism. These angiogenesis mechanisms may provide clues to develop potential therapeutic plans to regulate not only wound healing but also other pathological complications such as cancer, chronic inflammatory disorders, and cardiovascular diseases by precisely switching the IA.

Acknowledgement

This work was supported by research grant from Department of Science and Technology, Inspire Faculty Program, Government of India to S. Vimalraj (grant no. DST/INSPIRE/04/2017/002913) and this work was also supported by research grant from Science and Engineering Research Board (SERB), India to S. Vimalraj (grant no. PDF/2015/000133). This work was partially supported by a grant from the University Grant Commission-Faculty Research Program (UGC-FRP), Government of India and the Swiss National Science Foundation (SNSF) International Short Visit Programme in Professor Valentin Djonov's laboratory in the University of Bern.

Appendix A. Supplementary data

Supplementary data to this article can be found online at https://doi.org/10.1016/j.niox.2018.11.001.

References

[1] R.H. Tuhin, M. Begum, S. Rahman, R. Karim, T. Begum, S.U. Ahmed, R. Mostofa, A. Hossain, M. Abdel-Daim, R. Begum, Wound healing effect of Euphorbia hirta linn. (Euphorbiaceae) in alloxan induced diabetic rats, BMC Compl. Altern. Med. 17 (1) (2017) 423.
[2] R.F. Diegelmann, M.C. Evans, Wound healing: an overview of acute, fibrotic and delayed healing, Front. Biosci. 9 (2004) 283–289.
[3] T. Dinh, S. Braunagel, B.I. Rosenblum, Growth factors in wound healing: the present and the future? Clin. Podiatr. Med. Surg. 32 (1) (2015) 109–119.
[4] N.T. Bennett, G.S. Schultz, Growth factors and wound healing: Part II. Role in normal and chronic wound healing, Am. J. Surg. 166 (1) (1993) 74–81.
[5] C. Szabo, Gasotransmitters in cancer: from pathophysiology to experimental therapy, Nat. Rev. Drug Discov. 15 (3) (2016) 185–203.
[6] R. Weller, A.D. Ormerod, R.P. Hobson, N.J. Benjamin, A randomized trial of acidified nitrite cream in the treatment of tinea pedis, J. Am. Acad. Dermatol. 38 (4) (1998) 559–563.
[7] S. Vimalraj, V.N. Sumantran, S. Chatterjee, MicroRNAs: impaired vasculogenesis in metal induced teratogenicity, Reprod. Toxicol. 70 (2017) 30–48.
[8] A.D. Ormerod, M.I. White, S.A. Shah, N. Benjamin, Molluscum contagiosum effectively treated with a topical acidified nitrite, nitric oxide liberating cream, Br. J. Dermatol. 141 (6) (1999) 1051–1053.
[9] I. Shah, A. Petroczi, R.A. James, D.P. Naughton, Determination of nitrate and nitrite content of dietary supplements using ion chromatography, J. Anal. Bioanal. Tech. S12 (2013) 003, https://doi.org/10.4172/2155-9872.S12-003.
[10] S. Vimalraj, S. Bhuvaneswari, S. Lakshmikirupa, G. Jyothsna, S. Chatterjee, Nitric oxide signaling regulates tumor-induced intussusceptive-like angiogenesis, Microvasc. Res. 119 (2018) 47–59.
[11] R. Richardson, M. Metzger, P. Knyphausen, T. Ramezani, K. Slanchev, C. Kraus, E. Schmelzer, M. Hammerschmidt, Re-epithelialization of cutaneous wounds in adult zebrafish combines mechanisms of wound closure in embryonic and adult mammals, Development 143 (12) (2016) 2077–2088.
[12] M.J. Redd, L. Cooper, W. Wood, B. Stramer, P. Martin, Wound healing and inflammation: embryos reveal the way to perfect repair, Philos. Trans. R. Soc. Lond. B Biol. Sci. 359 (2004) 777–784.
[13] R. Weller, M.J. Finnen, The effects of topical treatment with acidified nitrite on wound healing in normal and diabetic mice, Nitric Oxide 15 (4) (2006) 395–399.
[14] R. Hlushchuk, D. Brönnimann, C. Correa Shokiche, L. Schaad, R. Triet, A. Jazwinska, S.A. Tschanz, V. Djonov, Zebrafish Caudal Fin Angiogenesis Assay-Advanced Quantitative Assessment Including 3-Way Correlative Microscopy, PLoS One 11 (3) (2016) e0149281.
[15] A. Suvik, A.W.M. Effendy, The use of modified masson's trichrome staining in collagen evaluation in wound healing study, Malays. J. Veterin. Res. 3 (1) (2012) 39–47.
[16] V. Prabhu, S.B. Rao, E.M. Fernandes, A.C. Rao, K. Prasad, K.K. Mahato, Objective assessment of endogenous collagen in vivo during tissue repair by laser induced fluorescence, PLoS One 9 (5) (2014) e98609.
[17] S. Vimalraj, N. Selvamurugan, MicroRNAs expression and their regulatory networks during mesenchymal stem cells differentiation toward osteoblasts, Int. J. Biol. Macromol. 66 (2014) 194–202.
[18] S. Vimalraj, N. Selvamurugan, Regulation of proliferation and apoptosis in human osteoblastic cells by microRNA-15b, Int. J. Biol. Macromol. 79 (2015) 490–497.
[19] S. Vimalraj, N.C. Partridge, N. Selvamurugan, A positive role of microRNA-15b on regulation of osteoblast differentiation, J. Cell. Physiol. 229 (9) (2014) 1236–1244.
[20] G.C. Gurtner, S. Werner, Y. Barrandon, M.T. Longaker, Wound repair and regeneration, Nature 453 (7193) (2008) 314–321.
[21] S. Barrientos, O. Stojadinovic, M.S. Golinko, H. Brem, M. Tomic-Canic, Growth factors and cytokines in wound healing, Wound Repair Regen. 16 (2008) 585–601.
[22] M.B. Witte, A. Barbul, Role of nitric oxide in wound repair, Am. J. Surg. 183 (4) (2002 Apr) 406–412.
[23] A. Karamercan, S. Ercan, S. Bozkurt, Nitric oxide synthase inhibitors appear to improve wound healing in endotoxemic rats: an investigator-blinded, controlled, experimental study, Curr. Ther. Res. Clin. Exp. 67 (6) (2006) 378–385.
[24] K. Verma, J. Gu, E. Werner, Tumor endothelial marker 8 amplifies canonical Wnt signaling in blood vessels, PLoS One 6 (8) (2011) e22334, , https://doi.org/10.1371/journal.pone.0022334.
[25] I. Dimova, V. Djonov, Role of Notch, SDF-1 and mononuclear cells recruitment in angiogenesis, Physiologic and Pathologic Angiogenesis - Signaling Mechanisms and Targeted Therapy, (2017), https://doi.org/10.5772/66761.
[26] I. Dimova, R. Hlushchuk, A. Makanya, B. Styp-Rekowska, A. Ceausu, S. Flueckiger, S. Lang, D. Semela, F. Le Noble, S. Chatterjee, V. Djonov, Inhibition of Notch signaling induces extensive intussusceptive neo-angiogenesis by recruitment of mononuclear cells, Angiogenesis 16 (4) (2013) 921–937.
[27] P.P. Zheng, W.C. Hop, P.A. Sillevis Smitt, M.J. van den Bent, C.J. Avezaat, T.M. Luider, J.M. Kros, Low-molecular weight caldesmon as a potential serum marker for glioma, Clin. Canc. Res. 11 (12) (2005) 4388–4392.
[28] P.P. Zheng, T.M. Luider, R. Pieters, C.J. Avezaat, M.J. van den Bent, P.A. Sillevis Smitt, J.M. Kros, Identification of tumor-related proteins by proteomic analysis of cerebrospinal fluid from patients with primary brain tumors, J. Neuropathol. Exp. Neurol. 62 (8) (2003) 855–862.
[29] P. Schlatter, M.F. Konig, L.M. Karlsson, P.H. Burri, Quantitative study of intussusceptive capillary growth in the chorioallantoic membrane (CAM) of the chicken embryo, Microvasc. Res. 54 (1997) 65–73.
[30] H. Kurz, S. Ambrosy, J. Wilting, D. Marme, B. Christ, Proliferation pattern of capillary endothelial cells in chorioallantoic membrane development indicates local growth control, which is counteracted by vascular endothelial growth factor application, Dev. Dynam. 203 (1995) 174–186.
[31] S.M. Paulsen, S.H. Wurster, L.B. Nanney, Expression of inducible nitric oxide synthase in human burn wounds, Wound Repair Regen. 6 (2) (1998 Mar-Apr) 142–148.
[32] E.A. Carter, T. Derojas-Walker, S. Tamir, S.R. Tannenbaum, Y.M. Yu, R.G. Tompkins, Nitric oxide production is intensely and persistently increased in tissue by thermal injury, J. Biochem. 304 (1994) 201–204.
[33] B. Wenezak, L.B. Nanney, Correlation of transforming growth factor-a and epidermal growth factor receptor with proliferating cell nuclear antigen in human burn wounds, Wound Repair Regen. 1 (1993) 219–230.
[34] J. Wruss, G. Waldenberger, S. Huemer, P. Uygun, P. Lanzerstorfer, U. Müller, O. Höglinger, J. Weghuber, Compositional characteristics of commercial beetroot products and beetroot juice prepared from seven beetroot varieties grown in Upper Austria, J. Food Compos. Anal. 42 (2015) 46–55.
[35] D. Kumar, B.G. Branch, C.B. Pattillo, J. Hood, S. Thoma, Simpson, W. Langston, Chronic sodium nitrite therapy augments ischemia-induced angiogenesis and arteriogenesis, Proc. Natl. Acad. Sci. Unit. States Am. 105 (21) (2008) 7540–7545.
[36] Z. Cao, L.D. Jensen, P. Rouhi, K. Hosaka, T. Länne, J.F. Steffensen, E. Wahlberg, Y. Cao, Hypoxia-induced retinopathy model in adult zebrafish, Nat. Protoc. 5 (12) (2010) 1903–1910.
[37] X.D. Chen, S.B. Ruan, Z.P. Lin, Z. Zhou, F.G. Zhang, R.H. Yang, J.L. Xie, Effects of porcine acellular dermal matrix treatment on wound healing and scar formation: role of Jag1 expression in epidermal stem cells, Organogenesis (2018) 1–11, https://doi.org/10.1080/15476278.2018.
[38] S. Patan, L.L. Munn, S. Tanda, S. Roberge, R.K. Jain, R.C. Jones, Vascular morphogenesis and remodeling in a model of tissue repair: blood vessel formation and growth in the ovarian pedicle after ovariectomy, Circ. Res. 89 (8) (2001) 723–731.
[39] J. Etulain, Platelets in wound healing and regenerative medicine, Platelets (2018

Feb 14) 1–13.
[40] S.B. Jakowlew, R. Lechleider, A.G. Geiser, S.J. Kim, T.A. Santa-Coloma, J. Cubert, M.B. Sporn, A.B. Roberts, Identification and characterization of the chicken transforming growth factor-beta 3 promoter, Mol. Endocrinol. 6 (8) (1992) 1285–1298.
[41] K. Fujio, T. Komai, M. Inoue, K. Morita, T. Okamura, K. Yamamoto, Revisiting the regulatory roles of the TGF-β family of cytokines, Autoimmun. Rev. 15 (9) (2016) 917–922.
[42] V. Saidkhani, M. Asadizaker, M.J. Khodayar, S.M. Latifi, The effect of nitric oxide releasing cream on healing pressure ulcers, Iran. J. Nurs. Midwifery Res. 21 (3) (2016) 322–330, https://doi.org/10.4103/1735-9066.180389.
[43] M. Rizzi, M. Migliario, S. Tonello, V. Rocchetti, F. Renò, Photobiomodulation induces in vitro re-epithelialization via nitric oxide production, Laser Med. Sci. (2018), https://doi.org/10.1007/s10103-018-2443-7.
[44] A. Shukla, A.M. Rasik, R. Shankar, Nitric oxide inhibits wounds collagen synthesis, Mol. Cell. Biochem. 200 (1–2) (1999) 27–33.
[45] M.A.1 Konerding, A. Turhan, D.J. Ravnic, M. Lin, C. Fuchs, T.W. Secomb, A. Tsuda, S.J. Mentzer, Inflammation-induced intussusceptive angiogenesis in murine colitis, Anat Rec (Hoboken) 293 (5) (2010 May) 849–857.
[46] S. Paku, K. Dezso, E. Bugyik, J. Tóvári, J. Tímár, P. Nagy, V. Laszlo, W. Klepetko, B. Döme, A new mechanism for pillar formation during tumor-induced intussusceptive angiogenesis: inverse sprouting, Am. J. Pathol. 179 (3) (2011 Sep) 1573–1585.
[47] B. Styp-Rekowska, R. Hlushchuk, A.R. Pries, V. Djonov, Intussusceptive angiogenesis: pillars against the blood flow, Acta Physiol (Oxf). 202 (3) (2011) 213–223.
[48] A.C. Taylor, L.M. Seltz, P.A. Yates, S.M. Peirce, Chronic whole-body hypoxia induces intussusceptive angiogenesis and microvascular remodeling in the mouse retina, MVR (Microvasc. Res.) 79 (2) (2010) 93–101, https://doi.org/10.1016/j.mvr.2010.01.006.
[49] E. Crivellato, B. Nico, A. Vacca, V. Djonov, M. Presta, D. Ribatti, Recombinant human erythropoietin induces intussusceptive microvascular growth in vivo, Leukemia 18 (2) (2004) 331–336.
[50] S.J. Mentzer, M.A. Konerding, Intussusceptive angiogenesis: expansion and remodeling of microvascular networks, Angiogenesis 17 (3) (2014) 499–509.
[51] L. Cooper, C. Johnson, F. Burslem, P. Martin, Wound healing and inflammation genes revealed by array analysis of "macrophageless" PU.1 null mice, Genome Biol. 6 (1) (2005) R5, https://doi.org/10.1186/gb-2004-6-1-r5.
[52] A.N. Makanya, R. Hlushchuk, V.G. Djonov, Intussusceptive angiogenesis and its role in vascular morphogenesis, patterning, and remodeling, Angiogenesis 12 (2) (2009) 113–123.
[53] W. De Spiegelaere, C. Casteleyn, W. Van den Broeck, J. Plendl, M. Bahramsoltani, P. Simoens, V. Djonov, P. Cornillie, Intussusceptive angiogenesis: a biologically relevant form of angiogenesis, J. Vasc. Res. 49 (5) (2012) 390–404.
[54] L. Díaz-Flores, R. Gutiérrez, M. Del Pino García, F.J. Sáez, L. Díaz-Flores Jr., J.F. Madrid, Piecemeal mechanism combining sprouting and intussusceptive angiogenesis in intravenous papillary formation induced by PGE2 and glycerol, Anat Rec (Hoboken) (2017), https://doi.org/10.1002/ar.23599.
[55] S. Patan, B. Haenni, P.H. Burri, Evidence for intussusceptive capillarygrowth in the chicken chorio-allantoic membrane (CAM), Anat. Embryol. 187 (1993) 121–130.
[56] A. Logothetidou, T. Vandecasteele, E. Van Mulken, K. Vandevelde, P. Cornillie, Intussusceptive angiogenesis and expression of Tie receptors during porcine metanephric kidney development, Histol. Histopathol. (2016) 11850.
[57] C. Van Steenkiste, B. Trachet, C. Casteleyn, D. van Loo, L. Van Hoorebeke, P. Segers, A. Geerts, H. Van Vlierberghe, I. Colle, Vascular corrosion casting: analyzing wall shear stress in the portal vein and vascular abnormalities in portal hypertensive and cirrhotic rodents, Lab. Invest. 90 (2010) 1558–1572.
[58] T.A. Petrie, N.S. Strand, C.T. Yang, J.S. Rabinowitz, R.T. Moon, Macrophages modulate adult zebrafish tail fin regeneration, Development 141 (13) (2014) 2581–2591.
[59] E. McNeill, M.J. Crabtree, N. Sahgal, et al., Regulation of iNOS function and cellular redox state by macrophage Gch1 reveals specific requirements for tetrahydrobiopterin in NRF2 activation, Free Radical Biol. Med. 79 (2015) 206–216.
[60] K.W. Zeng, L.X. Liao, H.N. Lv, F.J. Song, Q. Yu, X. Dong, J. Li, Y. Jiang, P.F. Tu, Natural small molecule FMHM inhibits lipopolysaccharide-induced inflammatory response by promoting TRAF6 degradation via K48-linked polyubiquitination, Sci. Rep. 5 (2015) 14715.
[61] L.C. Wang, L.X. Liao, H.N. Lv, D. Liu, W. Dong, J. Zhu, J.F. Chen, M.L. Shi, G. Fu, X.M. Song, Y. Jiang, K.W. Zeng, P.F. Tu, Highly selective activation of heat shock Protein 70 by allosteric regulation provides an insight into efficient neuroinflammation inhibition, EBioMedicine 23 (2017) 160–172.
[62] L.X. Liao, X.M. Song, L.C. Wang, H.N. Lv, J.F. Chen, D. Liu, G. Fu, M.B. Zhao, Y. Jiang, K.W. Zeng, P.F. Tu, Highly selective inhibition of IMPDH2 provides the basis of antineuroinflammation therapy, Proc. Natl. Acad. Sci. U. S. A. 114 (29) (2017) E5986–E5994.
[63] D. Tsikas, A. Bollenbach, E. Hanff, A.A. Kayacelebi, Asymmetric dimethylarginine (ADMA), symmetric dimethylarginine (SDMA) and homoarginine (hArg): the ADMA, SDMA and hArg paradoxes, Cardiovasc. Diabetol. 17 (1) (2018) 1.
[64] B. Weiss, Evidence for mutagenesis by nitric oxide during nitrate metabolism in Escherichia coli, J. Bacteriol. 188 (3) (2006) 829–833.
[65] T. Kitano, H. Yamada, M. Kida, Y. Okada, S. Saika, M. Yoshida, Impaired healing of a cutaneous wound in an inducible nitric oxide synthase-knockout mouse, Dermatol. Res. Pract. (2017) 2184040.